

## Interpersonal differences caused by adaptogen changes in the entropies of EEG, HRV, immunocytogram, and leukocytogram

OLEKSANDR POPADYNETS<sup>1</sup>, ANATOLIY GOZHENKO<sup>2</sup>, NATALIYA BADYUK<sup>3</sup>, IGOR POPOVYCH<sup>4</sup>,  
ALEXANDER SKALIY<sup>5</sup>, MAGDALENA HAGNER-DERENGOWSKA<sup>6</sup>, MAREK NAPIERAŁA<sup>7</sup>,  
RADOSŁAW MUSZKIETA<sup>8</sup>, DARIUSZ SOKOŁOWSKI<sup>9</sup>, WALERY ZUKOW<sup>10</sup>, LINA RYBALKO<sup>11</sup>

<sup>1,2,3,4</sup>Ukrainian Scientific Research Institute of Medicine for Transport, Odesa, UKRAINE

<sup>4</sup>OO Bohomolets' Institute of Physiology, Kyïv, UKRAINE

<sup>5</sup>University of Economy, Bydgoszcz, POLAND

<sup>6,8,9,10</sup>Nicolaus Copernicus University, Torun, POLAND

<sup>7</sup>Kazimierz Wielki University, Bydgoszcz, POLAND

<sup>11</sup>National University «Yuri Kondratyuk Poltava Polytechnic», Poltava, UKRAINE

Corresponding Author: ALEXANDER SKALIY, E-mail: skalii@wp.pl

Published online: February 20, 2020

(Accepted for publication: February 15, 2020)

DOI: 10.7752/jpes.2020.s....

### Abstract

**Background.** Previously, we have shown that in patients the entropy of HRV and spectral power density (SPD) of loci of EEG as well as of Immunocytogram (ICG) and Leukocytogram (LCG) is characterized by a large variation. The purpose of this study is to analyze variants of **changes** in entropy under the influence of natural adaptogens and to determine the possibility of their prediction. **Material and methods.** In basal conditions in 37 men and 14 women with dysfunction of neuro-endocrine-immune complex and metabolism, we recorded twice, before and after balneotherapy at the spa Truskavets', EEG ("NeuroCom Standard") and HRV ("Cardiolab+VSR"). In blood we determined relative content of components (RCC) of ICG (Th, Tc, B and NK lymphocytes) and LCG (Eosinophils, Stab and Segmentonuclear Neutrophils, Lymphocytes and Monocytes). Then we calculated for each locus of EEG and HRV as well as for ICG and LCG the Entropy (H) of normalized SPD or RCC using Shannon's formula. **Results.** Three clusters of persons were created. Balneotherapy has a generalized **negentropic** effect on EEG of 66,7% patients. The members of the other two clusters have substantially increased EEG entropy overall, but there are significant differences with respect to individual loci. The entropy changes of HRV, ICG, and LCG are within  $\pm 0,5 \sigma$ . The changes in entropy only 11 loci EEG and ICG were identified as characteristic of the clusters. It is shown that both the decrease in entropy in the first cluster and its increase in the third cluster (13,7% of patients) is normalizing. Instead, in the second cluster (19,6%), like the first cluster, only 4 EEG parameters change, whereas the entropy of most parameters rises above the upper limit of the norm, ie the true **proentropic** effect of balneotherapy takes place. The entropy change directionality is driven by 19 predictors, primarily the initial entropy levels of EEG, HRV, ICG, and LCG, as well as Popovych's Adaptation and Strain Indexes and gender, but not the age of the patients. **Conclusion.** Differentially directed entropy changes under the influence of natural adaptogens are, as a rule, normalizing in nature and predetermined by both its initial levels and other predictors.

**Key words:** EEG, HRV, Leukocytogram, Immunocytogram, Entropy, Balneotherapy, Clusters, Women and Man.

## Introduction

Previously, we have shown that in patients the entropy of HRV and SPD of loci of EEG as well as ICG and LCG is characterized by a large variation, which corresponds to the known wide variance of parameters of the ICG and LCG, which are subordinate to the regulatory influences of the central and autonomic nervous system (Popadynets' et al., 2019a; Popadynets' et al., 2019c). The method of cluster analysis is revealed that in members of the major cluster (60%), the entropy of EEG, HRV, ICG and LCG varies within the normal range ( $-0,5\sigma \div +0,5\sigma$ ). The members of the next largest cluster (23%) are characterized by a moderately increased entropy of the SPD of EEG in conjunction with the normal entropy of the ICG and the moderately reduced entropy of HRV and LCG. The members of the third cluster (9%) noted a significantly lower 43 entropy (negentropy) of the SPD in loci F3, F4, T3 and C4; in addition, there is a moderate decrease in the entropy of the LCG. Instead, members of the last cluster (8) noted the negentropy of SPD in paired loci Fp1 and Fp2, T5 and T6, T3 and T4, F7 and F8 as well as O1 and O2; in addition, there is a moderate decrease in entropy of the ICG. The entropy of other EEG locus as well as of HRV and LCG is within the normal range (Popadynets' et al., 2019).

Accepting the entropy (h) of EEG&HRV as a factors, using the correlation analysis with step-by-step exclusion, we obtain the equations for immune parameters as dependent variables. Canonical correlation between hEEG&HRV, on the one hand, and hLCG&Immunity, on the other hand, is strong:  $R=0,814$ ;  $R^2=0,663$ ;  $\chi^2_{(240)}=296$ ;  $p=0,008$  (Zukow et al., 2019). Thus, the entropy of EEG and HRV significantly correlate with the entropy and parameters of immunity, which testifies to their modulating regulatory effects.

The findings led us to seek answers to the question, do the **changes** in the SPD EEG entropy caused by external factors affect the immunity parameters?

The purpose of this preliminary study is to analyze variants of changes in entropy under the influence of balneofactors of Truskavets' spa as natural adaptogens (Kostyuk et al., 2006; Kozyavkina et al., 2015; Popovych, 2011) and to determine the possibility of their prediction.

## Material and methods

The object of observation were 37 men and 14 women aged 23-76 years old, who came to the spa Truskavets' (Ukraine) for the treatment of chronic pyelonephritis and cholecystitis in remission as well as without clinical diagnose but with dysfunction of neuro-endocrine-immune complex and metabolism. The survey was conducted twice, before and after standard balneotherapy (drinking bioactive water Naftussya three times a day, ozokerite applications, mineral baths every other day for 7-10 days) (Popovych, 2018; Popovych, 2019).

We recorded electrocardiogram in II lead (hardware-software complex "CardioLab+HRV" produced by "KhAI-MEDICA", Kharkiv) to assess the parameters of heart rate variability (HRV). For further analysis (Frequency Domain Methods) were selected normalized (%) spectral power (SP) bands of HRV: high-frequency (HF, range  $0,4 \div 0,15$  Hz), low-frequency (LF, range  $0,15 \div 0,04$  Hz), very low-frequency (VLF, range  $0,04 \div 0,015$  Hz) and ultra low-frequency (ULF, range  $0,015 \div 0,003$  Hz) (Baevskiy, 2001; Berntson et al., 1997; Heart Rate Variability, 1996).

Simultaneously we recorded EEG (hardware-software complex "NeuroCom Standard", KhAI Medica, Kharkiv) monopolar in 16 loci (Fp1, Fp2, F3, F4, F7, F8, C3, C4, T3, T4, P3, P4, T5, T6, O1, O2) by 10-20 international system, with the reference electrodes A and Ref on the tassels of ears. Among the options considered the normalized (%) spectral power density (SPD) in the standard frequency bands:  $\beta$  ( $35 \div 13$  Hz),  $\alpha$  ( $13 \div 8$  Hz),  $\theta$  ( $8 \div 4$  Hz) and  $\delta$  ( $4 \div 0,5$  Hz) in all loci, according to the instructions of the device.

We calculated for HRV and each locus EEG the Entropy (h) of normalized SPD using formulas (Popovych, 2007; Yushkovs'ka, 2001) based on CE Shannon's formula (Shannon, 1963):

$$hHRV = - [SPDHF \cdot \log_2 SPDHF + SPDLF \cdot \log_2 SPDLF + SPDVLF \cdot \log_2 SPDVLF + SPDULF \cdot \log_2 SPDULF] / \log_2 4;$$

$$hEEG = - [SPD\alpha \cdot \log_2 SPD\alpha + SPD\beta \cdot \log_2 SPD\beta + SPD\theta \cdot \log_2 SPD\theta + SPD\delta \cdot \log_2 SPD\delta] / \log_2 4$$

In portion of capillary blood we counted up Leukocytogram (LCG) (Eosinophils, Stub and Segmentonuclear Neutrophils, Lymphocytes and Monocytes) and calculated two variants of Adaptation Index as well as two variants of Strain Index by IL Popovych (Barylyak et al., 2013; Petsyukh et al. 2016).

$$\text{Strain Index-1} = [(Eo/3,5-1)^2 + (SN/3,5-1)^2 + (Mon/5,5-1)^2 + (Leu/6-1)^2]/4$$

$$\text{Strain Index-2} = [(Eo/2,75-1)^2 + (SN/4,25-1)^2 + (Mon/6-1)^2 + (Leu/5-1)^2]/4$$

Immune status evaluated on a set of I and II levels recommended by the WHO as described in the manual (Lapovets' & Lutsyk, 2002). For phenotyping subpopulations of lymphocytes used the methods of rosette formation with sheep erythrocytes on which adsorbed monoclonal antibodies against receptors CD3, CD4, CD8, CD22 and CD56 from company "Granum" (Kharkiv) with visualization under light microscope with immersion system.

We calculated also the Entropy (h) of Immunocytogram (ICG) and LCG using formulas:

$$hICG = - [CD4 \cdot \log_2 CD4 + CD8 \cdot \log_2 CD8 + CD22 \cdot \log_2 CD22 + CD56 \cdot \log_2 CD56] / \log_2 4$$

$$hLCG = - [Lymph \cdot \log_2 Lymph + Mon \cdot \log_2 Mon + Eos \cdot \log_2 Eos + SNN \cdot \log_2 SNN + StubN \cdot \log_2 StubN] / \log_2 5$$

Results processed using the software package "Statistica 5.5".

## Results

In the first stage, following the previously created algorithm (Popadynets' et al., 2019b), a cluster analysis of the entropy changes of EEG, HRV, ICG, and LCG was performed using the k-mean clustering (Aldenderfer & Blashfield, 1989) method. As a result, three groups of persons were created, significantly different from each other in terms of entropy changes (Table 1), while the differences between the members of each group were much smaller (Table 2).

**Table 1. Euclidean Distances between Clusters**

Distances below diagonal

Squared distances above diagonal

Cluster	No. 1	No. 2	No. 3
No. 1		,039	,040
No. 2	,196		,024
No. 3	,200	,156	

**Table 2. Members of Clusters and Distances from Respective Cluster Center**

Cluster Number 1 contains 34 cases

Case No	C_1	C_4	C_5	C_7	C_9	C_10	C_11	C_12	C_14	C_15	C_17	C_18
Distance	,159	,225	,379	,103	,095	,062	,125	,072	,061	,175	,112	,075
Case No	C_19	C_20	C_21	C_23	C_24	C_25	C_26	C_27	C_28	C_33	C_35	C_38
Distance	,142	,061	,342	,251	,064	,185	,143	,053	,097	,061	,152	,094

Case No	C_39	C_40	C_42	C_44	C_45	C_46	C_48	C_49	C_50	C_51		
Distance	,116	,111	,162	,101	,071	,129	,271	,064	,061	,069		

Cluster Number 2 contains 10 cases

Case No	C_2	C_3	C_6	C_16	C_22	C_29	C_34	C_36	C_37	C_47
Distance	,140	,107	,270	,112	,117	,120	,094	,236	,135	,148

Cluster Number 3 contains 7 cases

Case No	C_8	C_13	C_30	C_31	C_32	C_41	C_43
Distance	,122	,164	,153	,220	,126	,125	,153

The maximum contributions to the distribution of individuals, more precisely the changes in their entropy, to the clusters give changes in the entropy of SPD at loci C3 and C4, the minimal but significant contributions give changes in the loci of F8 and T6, while the contributions of entropy changes in ICG, LCG and HRV are not significant (Table 3).

**Table 3. Analysis of Variance for Changes in Entropy (H)**

Change in Variables	Between SS	Within SS	$\eta^2$	R	F	signif. p
C3H	,584	,552	0,514	0,717	25,4	10 <sup>-6</sup>
C4H	,650	,758	0,462	0,679	20,6	10 <sup>-6</sup>
O1H	,867	1,174	0,425	0,652	17,7	10 <sup>-5</sup>
Fp2H	,751	1,314	0,364	0,603	13,7	10 <sup>-4</sup>
P3H	,292	,567	0,340	0,583	12,4	10 <sup>-4</sup>
O2H	,539	1,172	0,315	0,561	11,0	10 <sup>-3</sup>
F3H	,340	,770	0,306	0,553	10,6	10 <sup>-3</sup>
F4H	,557	1,453	0,277	0,526	9,20	10 <sup>-3</sup>
F7H	,961	2,551	0,274	0,523	9,04	10 <sup>-3</sup>
P4H	,253	,789	0,243	0,493	7,68	,001
T5H	,534	1,677	0,242	0,491	7,65	,001
T4H	,412	1,314	0,239	0,489	7,53	,001
Fp1H	,523	1,672	0,238	0,488	7,51	,001
T3H	,416	1,400	0,229	0,479	7,13	,002
F8H	,885	3,250	0,214	0,463	6,54	,003
T6H	,486	1,805	0,212	0,461	6,47	,003
ICG H	,003	,036	0,077	0,277	1,75	,185

LCG H	,004	,127	0,031	0,175	,72	,494
HRV H	,014	,708	0,019	0,139	,49	,618

In Fig. 1 shows the profiles of changes in the actual entropy values for individuals of different clusters, and in Fig. 2 shows the profiles of changes in normalized values.

As can be seen, individuals in the major **first cluster** (66,7% of the cohort) are characterized by a moderate and approximately equal decrease in SPD entropy at all EEG loci in the absence of significant changes in HRV, ICG, and LCG entropy.

In individuals in the **second cluster** (19,6% of the cohort), the scope for the absence of significant entropy changes in HRV, ICG and LCG is supplemented by loci C4, C3, F3, F4, T4 and T3, and in the other 10 loci the entropy level is moderately increased.

In members of the **third cluster** (13,7% of the cohort), with the similar entropy stability of HRV, ICG and LCG, balneotherapy does not significantly affect the entropy of SPD at F8 and O2 loci, increasing it at Fp2, T6, O1 loci to a lesser extent than in the second. clusters, at the F7, T5, Fp1, P3, P4, and T4 loci are almost similar, and at the T3, F4, F3, C3, and C4 loci are much more pronounced. The integral proentropic effect of balneotherapy is greater in the members of the third cluster, but insignificantly (Fig. 3).

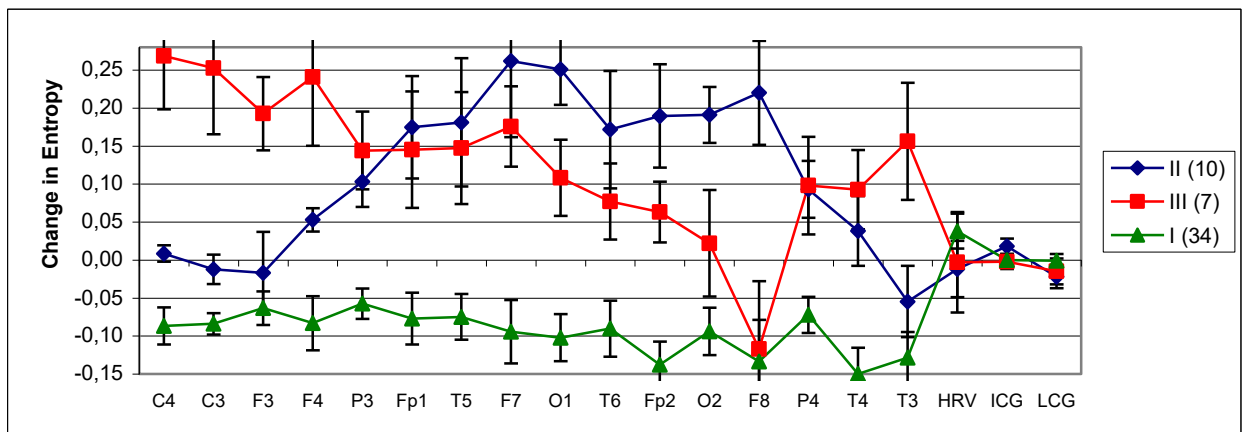


**Fig. 1. Actual mean values ( $M \pm SE$ ) of changes in the entropy of SPD in loci of EEG as well as of HRV, LCG and ICG in members of different clusters**

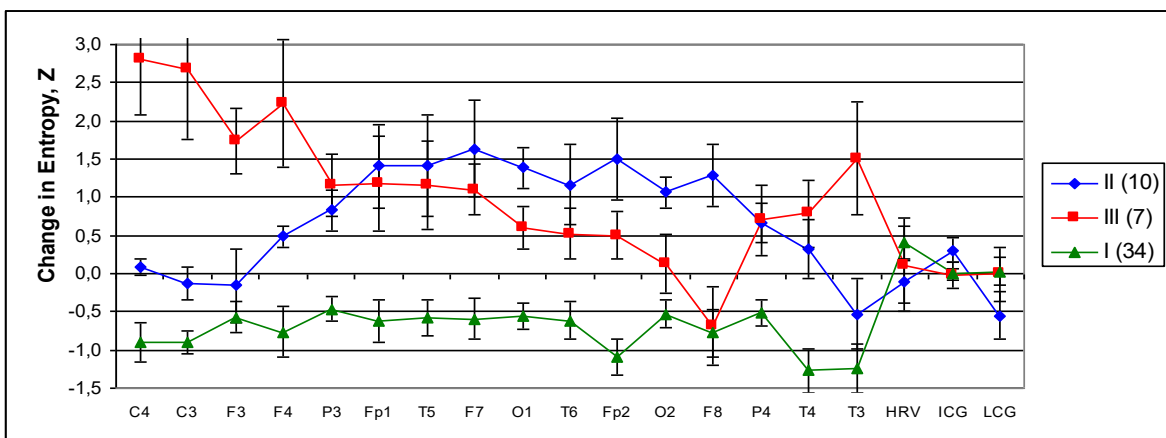


**Fig. 2. Z-scores (M±SE) of changes in the entropy of SPD in loci of EEG as well as of HRV, LCG and ICG in members of different clusters**

Therefore, balneotherapy has a generalized negentropic effect on EEG of 2/3 patients. On the other hand, the members of the other two clusters have substantially increased EEG entropy overall, but there are significant differences with respect to individual loci. The entropy changes of HRV, ICG, and LCG are within  $\pm 0,5 \sigma$ , which we consider to be insignificant.

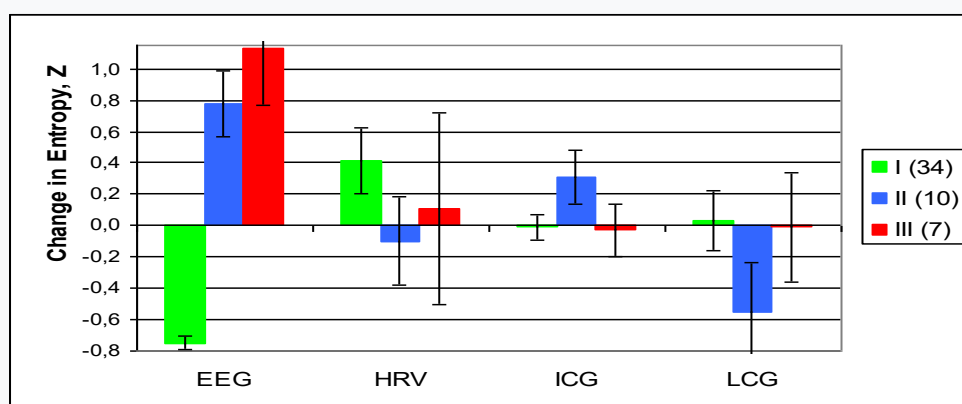


**Fig. 3. Changes in normalized entropy of SPD of loci of EEG, HRV, Immunocytogram and Leukocytogram in members of different clusters**

According to the results of the discriminant analysis (method forward stepwise [14]), changes in entropy only 11 loci EEG and ICG were identified as characteristic of the clusters. The other 5 loci of EEG as well as changes in entropy of LCG and HRV were not included in the discriminant model (Tables 4 and 5).

**Table 4. Discriminant Function Analysis Summary for Changes in Variables of Entropy in Clusters**

Step 12, N of vars in model: 12; Grouping: 3 grps

Wilks' Lambda: 0,119; approx.  $F_{(24,7)}=5,8$ ;  $p < 10^{-6}$

Variables currently in the model	Cluster No. 3 (7)	Cluster No.1 (34)	Cluster No.2 (10)	Wilks' $\Lambda$	Partial $\Lambda$	F-re-move	p-level	Tolerance
C3H	,253	-,065	-,012	,178	,670	9,10	,001	,432
C4H	,269	-,065	,009	,121	,991	,17	,842	,470
F4H	,241	-,060	,053	,146	,818	4,10	,025	,224
T3H	,156	-,111	-,055	,124	,960	,78	,466	,626
P3H	,144	-,039	,103	,152	,786	5,05	,012	,435
T4H	,093	-,127	,038	,132	,907	1,89	,165	,553
O1H	,108	-,071	,251	,140	,852	3,22	,051	,386

Fp2H	,063	-,108	,190	,129	,924	1,52	,231	,185
T5H	,147	-,049	,181	,134	,890	2,28	,116	,330
Fp1H	,145	-,052	,175	,125	,957	,83	,442	,295
F8H	-,117	-,111	,220	,131	,910	1,82	,176	,433
ICG H	-,002	-,000	,018	,124	,966	,66	,525	,781
Variables currently not in the model	<b>Cluster No. 3 (7)</b>	<b>Cluster No.1 (34)</b>	<b>Cluster No.2 (10)</b>	Wilks' $\Lambda$	Parti- al $\Lambda$	F to enter	p- level	Tole- rancy
F3H	,193	-,049	-,017	,114	,958	,79	,460	,608
F7H	,176	-,060	,262	,116	,973	,50	,610	,550
T6H	,077	-,066	,172	,119	1,000	,00	,995	,282
P4H	,098	-,054	,093	,118	,988	,22	,805	,476
O2H	,022	-,071	,191	,116	,976	,45	,643	,533
LCG H	-,015	-,001	-,022	,119	,997	,06	,941	,835
HRV H	,011	,030	-,012	,116	,974	,49	,619	,789

**Table 5. Summary of Stepwise Analysis for Changes in Entropy, ranked by criterion Lambda**

Changes in Variables	F to enter	p- level	$\Lambda$	F- value	p- level
C3H	25,4	$10^{-6}$	,486	25,4	$10^{-6}$
O1H	14,8	$10^{-5}$	,298	19,5	$10^{-6}$
T3H	3,8	,030	,256	15,0	$10^{-6}$
ICG H	3,0	,060	,226	12,4	$10^{-6}$
C4H	2,2	,122	,206	10,6	$10^{-6}$
P3H	1,5	,228	,192	9,2	$10^{-6}$
T4H	1,3	,273	,180	8,1	$10^{-6}$
F8H	2,7	,077	,159	7,7	$10^{-6}$
F4H	1,2	,302	,150	7,0	$10^{-6}$
Fp1H	1,7	,191	,138	6,6	$10^{-6}$
T5H	1,2	,300	,129	6,2	$10^{-6}$
Fp2H	1,5	,231	,119	5,8	$10^{-6}$

The 12-dimensional space of discriminant variables transforms into 2-dimensional space of a canonical roots. The canonical correlation coefficient is for Root 1 0,839 (Wilks'  $\Lambda=0,119$ ;  $\chi^2_{(24)}=90$ ;  $p<10^{-6}$ ), for Root 2 0,773

(Wilks'  $\Lambda=0,402$ ;  $\chi^2_{(11)}=39$ ;  $p<10^{-6}$ ). The major root contains 61,5% of discriminative capabilities, the minor contains 38,5%.

The calculation of the discriminant root values for each person as the sum of the products of raw coefficients to the individual values of discriminant variables together with the constant (Table 6) enables the visualization of each patient in the information space of the roots (Fig. 1).

**Table 6. Standardized and Raw Coefficients and Constants for Changes in Variables**

Coefficients	Standardized		Raw	
	Root 1	Root 2	Root 1	Root 2
Variables	Root 1	Root 2	Root 1	Root 2
C3H	-1,003	,306	-9,345	2,848
O1H	-,010	-,802	-,063	-5,127
T3H	-,300	,049	-1,756	,286
ICGH	,071	-,260	2,560	-9,425
C4H	-,117	-,130	-,931	-1,035
P3H	,378	-,811	3,478	-7,460
T4H	-,216	-,475	-1,308	-2,871
F8H	,466	,302	1,791	1,159
F4H	-,670	,909	-3,853	5,225
Fp1H	,450	-,079	2,413	-,425
T5H	-,340	,649	-1,817	3,470
Fp2H	,191	-,803	1,155	-4,850
	<b>Constants</b>		-,237	-,082
	<b>Eigenvalues</b>		2,370	1,485
<b>Cumulative Properties</b>			,615	1,000



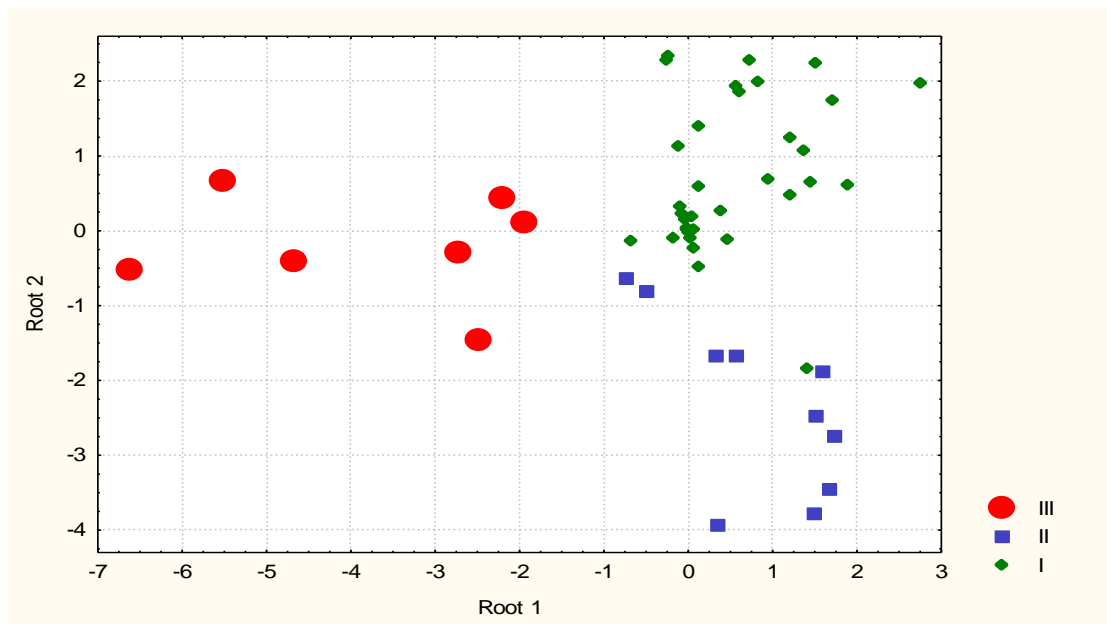


**Fig. 4. Individual values of the two roots of the changes in entropy of the members of the three clusters**

As you can see, all three clusters are quite clearly separated from each other. The visual impression is documented by the computation of Mahalanobis distances between clusters (Table 7).

**Table 7. Squared Mahalanobis Distances between changes in Entropy for Clusters, F-values (df=12,4) and p-levels**

Clusters	III	I	II
III	0	20	27
I	6,6 <math><10^{-5}</math>	0	10
II	6,1 <math><10^{-5}</math>	4,5 <math><10^{-3}</math>	0

Table 8 shows the correlation coefficients of entropy changes (discriminant variables) with canonical discriminant roots, the cluster centroids of both roots, and the normalized entropy change values of the discriminant variables, as well as not included in the discriminant model.

**Table 8. Correlations Variables-Canonical Roots, Means of Roots and Z-scores of changes in Variables for Clusters**

Change in Variables	Correlations Variables-Roots		III (7)	I (34)	II (10)
	R1	R2			
Root 1 (61,5%)			-3,74	+0,53	+0,80
C3H	-,645	-,219	+2,68	-0,89	-0,13

C4H	<b>-,569</b>	-,245	<b>+2,82</b>	-0,91	+0,09
F4H	<b>-,352</b>	-,246	<b>+2,21</b>	-0,77	+0,49
T3H	<b>-,336</b>	-,139	<b>+1,51</b>	-1,24	-0,53
P3H	<b>-,294</b>	-,457	<b>+1,16</b>	-0,46	+0,83
T4H	<b>-,235</b>	-,351	<b>+0,78</b>	-1,27	+0,32
F3H	currently not in model		<b>+1,74</b>	-0,57	-0,15
<b>Root 2 (38,5%)</b>	R1	R2	-0,21	<b>+0,72</b>	<b>-2,31</b>
O1H	-,118	<b>-,690</b>	+0,60	<b>-0,56</b>	<b>+1,38</b>
Fp2H	-,111	<b>-,604</b>	+0,50	<b>-1,10</b>	<b>+1,51</b>
T5H	-,154	<b>-,420</b>	+1,15	<b>-0,59</b>	<b>+1,42</b>
Fp1H	-,157	<b>-,414</b>	+1,17	<b>-0,62</b>	<b>+1,41</b>
F8H	,096	<b>-,411</b>	-0,68	<b>-0,78</b>	<b>+1,29</b>
ICG H	,057	<b>-,209</b>	-0,03	<b>-0,01</b>	<b>+0,31</b>
F7H	currently not in model		+1,10	<b>-0,59</b>	<b>+1,64</b>
T6H	currently not in model		+0,52	<b>-0,61</b>	<b>+1,16</b>
P4H	currently not in model		+0,70	<b>-0,52</b>	<b>+0,66</b>
O2H	currently not in model		+0,12	<b>-0,53</b>	<b>+1,06</b>
HRV H	currently not in model		+0,11	<b>+0,41</b>	<b>-0,10</b>
LCG H	currently not in model		-0,01	<b>+0,10</b>	<b>-0,55</b>

The localization of the members of the **third cluster** in the extremely left zone of the axis of the first root (Fig. 4) reflects the maximum for sampling the growth of SPD EEG entropy at the loci that represent the root inversely. The members of the other two clusters are localized in the opposite zone of the axis and are practically unbound, reflecting the absence of clear differences between the quasi-zero entropy changes.

At the same time, these clusters are clearly delineated along the axis of the second root. In particular, the lower zone is occupied by a **second cluster**, reflecting a significant increase in the entropy of SPD EEG at loci that represent the root inversely. Instead, the members of the **first cluster** are localized in the upper zone of the axis, reflecting a moderate decrease in entropy at these loci.

The use of the values of the centroids of the clusters for the labeling of the abscissa axis, and for the ordinate axis of the normalized mean values of the entropy changes makes it possible to visualize their patterns (Figs. 5 and 6).

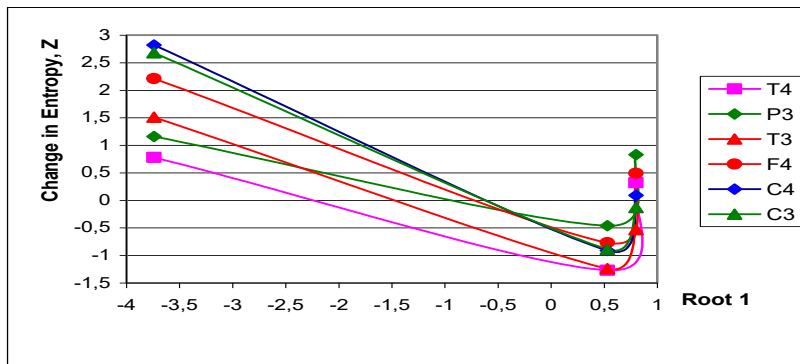


Fig. 5. The pattern of changes in the entropy of SPD EEG at the loci that represent the first root

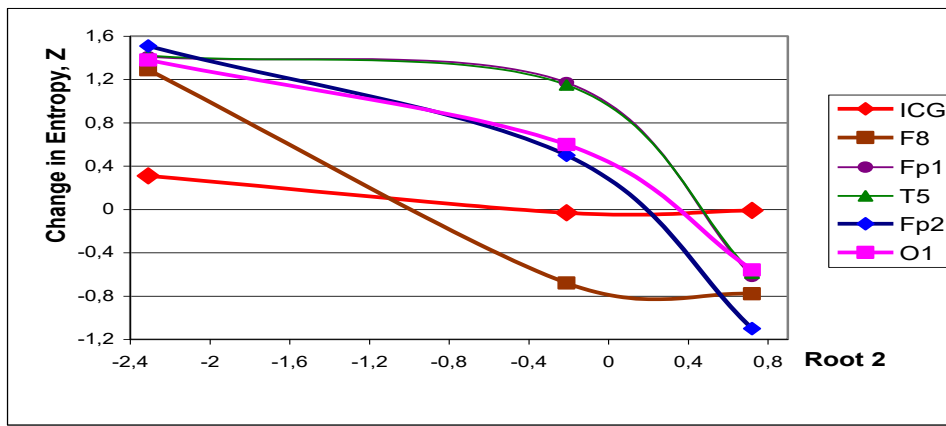


Fig. 6. The pattern of changes in the entropy of ICG and SPD EEG at the loci that represent the second root

In Fig. 7 shows the mean values of both roots (the abscissa axis) and the mean entropy changes (ordinate) for the three clusters. In this case, thick lines contain information about variables included in the discriminant model, and thin lines refer to variables not included in the model. As we can see, for each root they are almost indistinguishable.

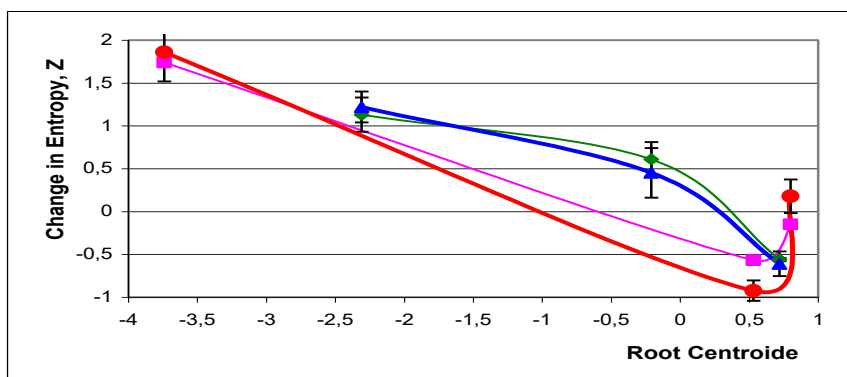


Fig. 7. Patterns of integral Entropy Changes for first and second Roots

The calculation of the classification functions by the coefficients and constants given in Table 9 allows us to retrospectively identify the members of the third cluster without error, the first cluster with one error and the second cluster with two errors (Table 10).

**Table 9. Coefficients and Constants for Classification Functions for Changes in Entropy**

Clusters	III	I	II
<b>Variables</b>	p=,137	p=,667	p=,196
C3H	31,48	-5,746	-16,92
O1H	4,249	-,801	14,72
T3H	1,333	-5,896	-7,240
ICG H	5,526	7,664	36,91
C4H	4,459	-,479	2,403
P3H	-12,67	-4,784	18,76
T4H	3,253	-5,006	3,335
F8H	-7,201	1,523	-1,501
F4H	16,81	5,237	-11,64
Fp1H	-5,110	4,792	6,738
T5H	10,108	5,589	-5,420
Fp2H	-11,81	-11,40	3,608
<b>Constants</b>	-8,576	-1,487	-5,111

**Table 10. Classification Matrix for Changes in Entropy**

Rows: Observed classifications; Columns: Predicted classifications

Clusters	Percent correct	III	II	I
		p=,137	p=,196	p=,667
III	100	<b>7</b>	0	0
II	80,0	0	<b>8</b>	<b>2</b>

I	97,1	0	<b>1</b>	<b>33</b>
Total	94,1	7	9	35

Now let's try to give a qualitative physiological assessment of the detected changes in the entropy of SPD of EEG loci. The petal diagrams give a general impression (Figs. 8-10), and more detailed information is provided by Fig. 11.

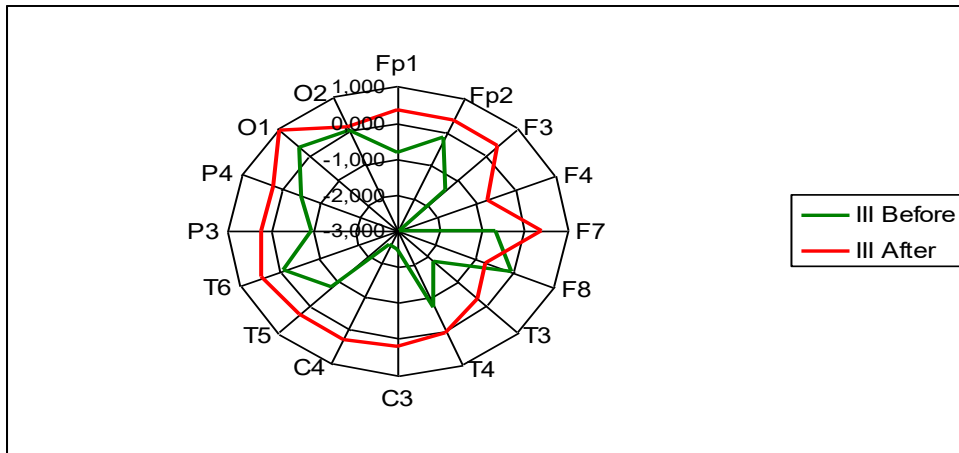


**Fig. 8. Petal diagram of entropy of SPD of EEG loci before and after balneotherapy in members of the third cluster**

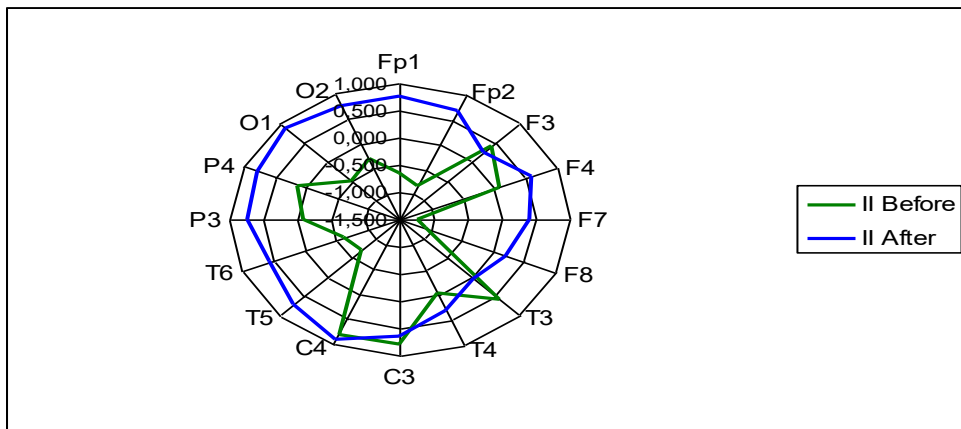


**Fig. 9. Petal diagram of entropy of SPD of EEG loci before and after balneotherapy in members of the second cluster**

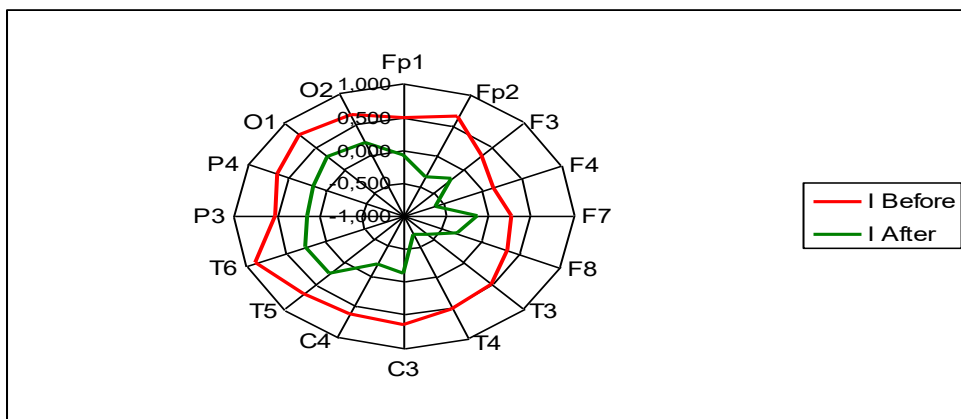


**Fig. 10. Petal diagram of entropy of SPD of EEG loci before and after balneotherapy in members of the first cluster**

As we can see, in the members of the **third cluster** increase both the reduced and the lower boundary entropy levels of SPD of 15 loci out of 16 registered, with 13 loci up to a range of  $-0,5 \div +0,5 \sigma$ , which we adopted as a narrowed norm. On the other hand, in the members of the **first cluster**, the upper boundary and moderately elevated entropy levels decrease to a narrowed area or slightly below. In general, both the increase in the initially significantly reduced entropy in the **third cluster** individuals and the decrease in the initially moderately increased entropy level in the **first cluster** individuals are normalizing (Fig. 12). In other words, 80,4% of patients have EEG entropy changes according to the classic “initial level law” (Balanovs’kyi, 1993, Kolyada, 1995).

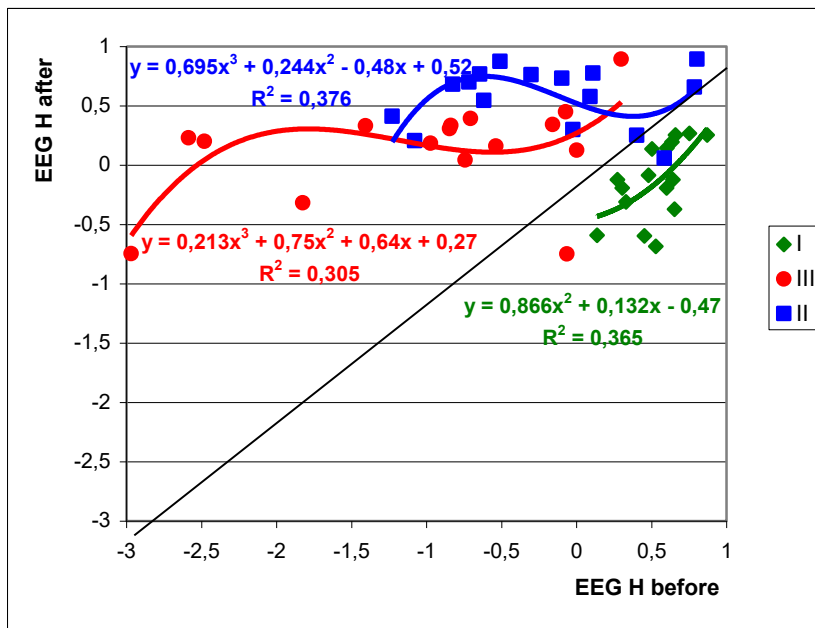


Fig. 11. Normalized mean entropy levels of SPD of EEG loci before (X-axis) and after (Y-axis) balneotherapy in members of different clusters

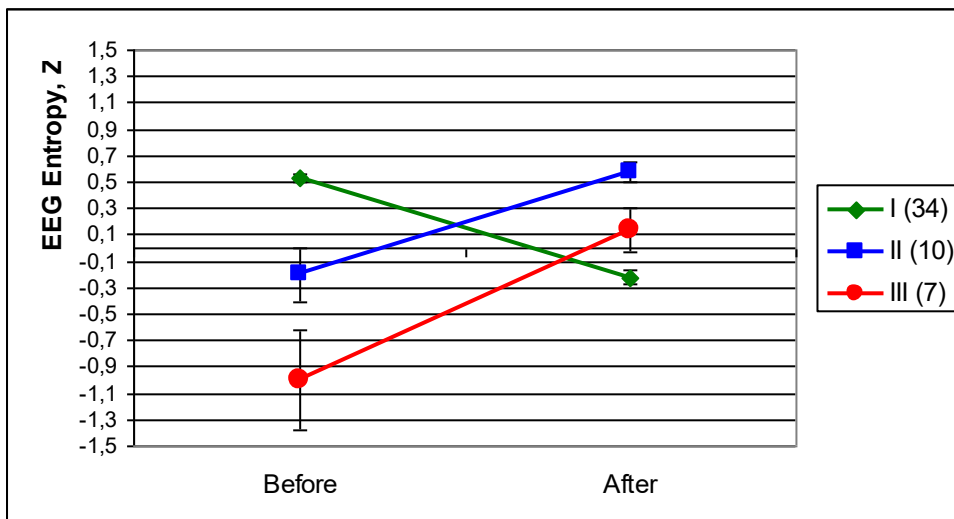


Fig. 12. Normalized integral entropy levels of EEG before and after balneotherapy in members of different clusters

Normalizing effect on body parameters deviated from the norm is considered one of the attributes of classical plant adaptogens (ginseng, eleutherococcus, rhodiola, etc.) (Kostyuk, 2006; Popovych, 2008). The Truskavetsian Scientific School has revealed the normalizing effects of balneotherapeutic complex in general and in particular of bioactive water Naftussya as its major components on the parameters of exchange of electrolytes and lipids, gastric and pancreatic secretion, cholekinetics, central and peripheral hemodynamic, physical work capacity, endocrine, immune and autonomic nervous systems (Balanovs'kyi et al., 1993; Chebanenko et al., 1997; Chebanenko et al., 2012; Gumega et al., 2011; Ivassivka et al., 2008a; Ivassivka et al., 2008b; Kostyuk et al., 2006; Kozyavkina, 2009; Kozyavkina, 2012; Kozyavkina et al., 2013a; Kozyavkina et al., 2013b; Kozyavkina et

al., 2015; Kul'chyns'kyi et al., 2017; Popovych, 2018; Popovych, 2019; Popovych, 2007; Popovych, et al., 2016; Popovych & Kozhavkina, 2012; Popovych, et al., 2018; Popovych et al., 2017; Popovych et al., 2005; Popovych et al., 2014; Ruzhylo, 2003, Sydoruk, et al., 2017).

It is these balneological effects, together with their stress limiting effect similar to that of phytoadaptogens, that have made them a class of adaptogens (Popovych, 2008; Popovych, 2011).

It is also known that parameters of the immune and autonomic nervous systems respond to the hypoxia, hypothermia, hyperthermia under the “initial level law” (Kolyada et al., 1995).

Instead, in the **second cluster**, like the first cluster, only 4 EEG parameters change, whereas the entropy of most parameters rises above the upper limit of the norm, ie the true proentropic effect of balneotherapy takes place. Similar excessive effects of balneotherapy have been observed previously with regard to the parameters of autonomous regulation and have been interpreted by the authors as a manifestation of a reactivity disorder (Gozhenko, 2004; Gozhenko, 2010; Kozhavkina et al., 2015).

The entropy responses of HRV (Figs. 13 and 14), ICG (Figs. 15 and 16), and LCG (Figs. 17 and 18) also occur under “entry-level law” but they are little expressed, especially against the backdrop of EEG entropy changes.

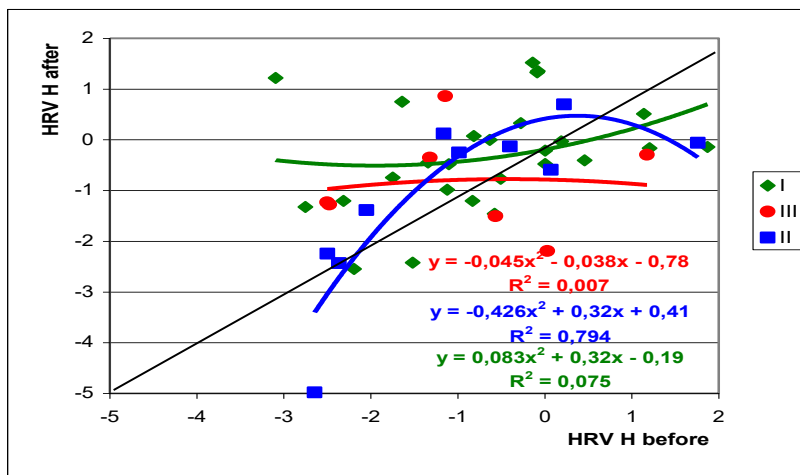


Fig. 13. Normalized mean entropy levels of HRV before (X-axis) and after (Y-axis) balneotherapy in members of different clusters

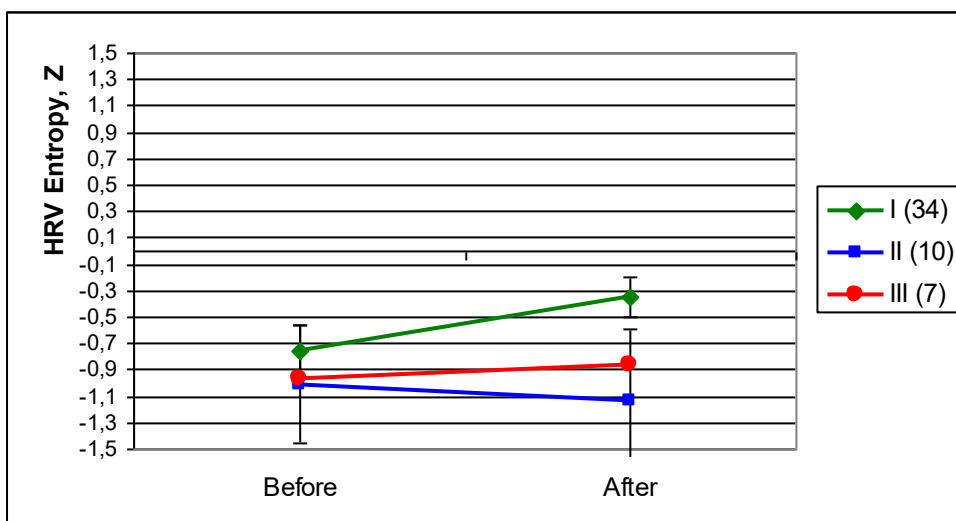




Fig. 14. Normalized integral entropy levels of HRV before and after balneotherapy in members of different clusters

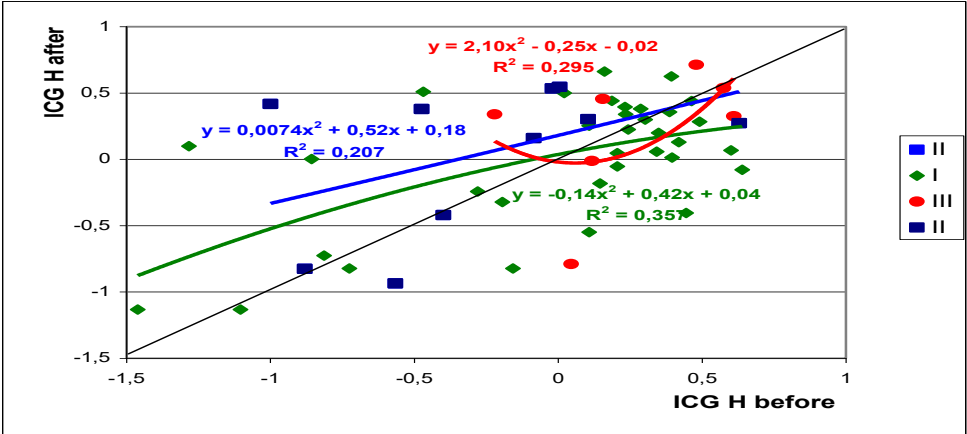


Fig. 15. Normalized mean entropy levels of ICG before (X-axis) and after (Y-axis) balneotherapy in members of different clusters

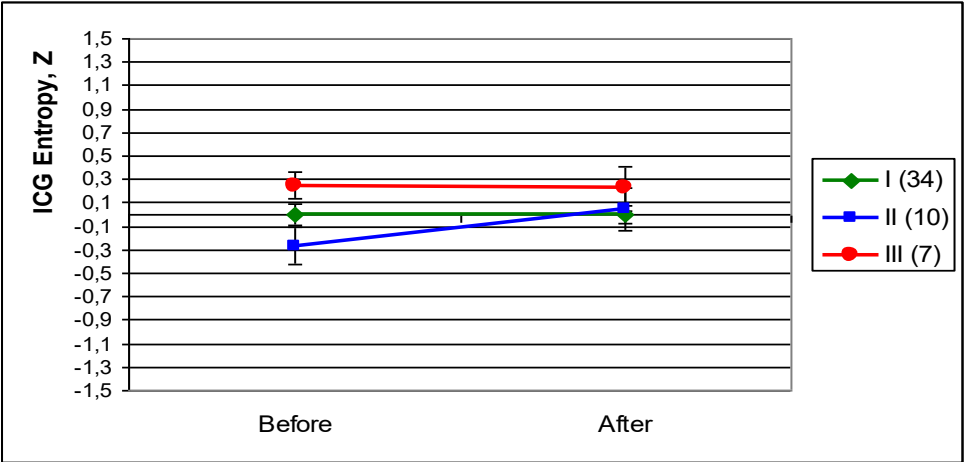


Fig. 16. Normalized integral entropy levels of ICG before and after balneotherapy in members of different clusters

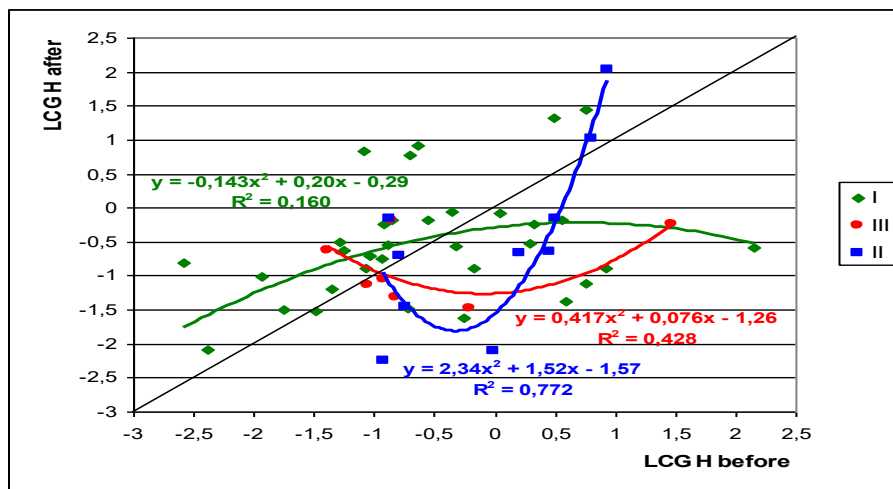


Fig. 17. Normalized mean entropy levels of LCG before (X-axis) and after (Y-axis) balneotherapy in members of different clusters

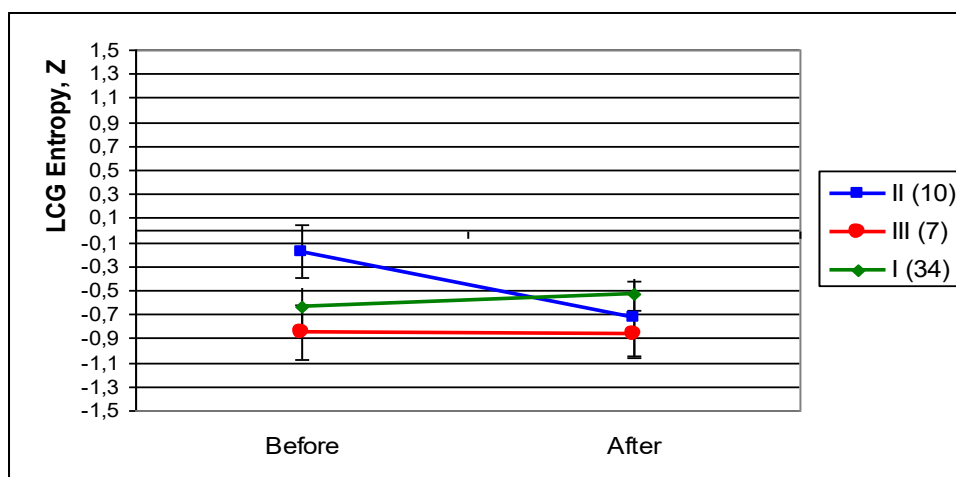


Fig. 18. Normalized integral entropy levels of LCG before and after balneotherapy in members of different clusters

It follows from the foregoing that the directionality of entropy responses to balneotherapy is due to its initial levels. Indeed, the discriminant analysis program selected **entropy of SPD** 12 from 16 EEG loci as well as **ICG**, **LCG** and **HRV** as predictors. In addition, both variants of **Popovych's Strain Index** of LCG and second but not the first variant of **Popovych's Adaptation Index** of LCG were well predicted as well as **gender** but not **age** of patients (Tables 11 and 12).

Table 11. Discriminant Function Analysis Summary for initial Variables, their actual Levels for Clusters as well as Norm and Coefficients of Variability

Step 19, N of vars in model: 19; Grouping: 3 grps. Wilks' Lambda: 0,041; approx.  $F_{(38,6)}=6,2$ ;  $p < 10^{-6}$

Variables currently in the model	II (10)	I (34)	III (7)	Wilks' Λ	Parti- al Λ	F-re- move (2,3)	p- level	Tole- rancy	Norm level (88)	Cv
<b>C4H</b>	0,907	0,887	0,583	,046	,906	1,57	,226	,233	0,830	0,115
<b>C3H</b>	0,901	0,888	0,593	,045	,913	1,43	,256	,160	0,827	0,114
<b>F4H</b>	0,838	0,843	0,506	,054	,763	4,65	,017	,316	0,828	0,131
<b>T3H</b>	0,884	0,870	0,634	,049	,837	2,92	,069	,231	0,823	0,126
<b>F3H</b>	0,855	0,844	0,654	,062	,662	7,66	,002	,217	0,810	0,137
<b>Sex Index</b>	1,50	1,24	1,14	,054	,763	4,65	,017	,341	1,5	0,250
<b>ICG H</b>	0,945	0,960	0,974	,048	,864	2,36	,112	,407	0,960	0,059
<b>PSI-2</b>	0,301	0,198	0,140	,047	,881	2,02	,150	,157	0,065	0,618
<b>LCG H</b>	0,672	0,651	0,641	,049	,837	2,91	,070	,445	0,681	0,070
<b>O1H</b>	0,581	0,818	0,736	,045	,928	1,16	,326	,235	0,682	0,266
<b>Fp2H</b>	0,678	0,864	0,762	,047	,879	2,06	,145	,269	0,782	0,161
<b>F7H</b>	0,576	0,816	0,659	,061	,674	7,26	,003	,193	0,772	0,207
<b>F8H</b>	0,572	0,813	0,746	,057	,725	5,68	,008	,130	0,757	0,226
<b>O2H</b>	0,634	0,802	0,688	,048	,856	2,52	,097	,193	0,688	0,261
<b>T4H</b>	0,806	0,871	0,721	,054	,759	4,76	,016	,322	0,809	0,146
<b>P4H</b>	0,776	0,845	0,686	,047	,880	2,04	,148	,243	0,761	0,184
<b>HRV H</b>	0,687	0,712	0,691	,046	,906	1,55	,228	,463	0,788	0,127
<b>PAI-2</b>	0,86	0,70	0,91	,044	,937	1,00	,379	,569	1,70	0,147
Variables currently not in the model	II (10)	I (34)	III (7)	Wilks' Λ	Parti- al Λ	F to enter	p- level	Tole- rancy	Norm level (88)	Cv
<b>T6H</b>	0,651	0,871	0,731	,041	,989	,16	,849	,240	0,742	0,199
<b>PAI-1</b>	1,27	1,10	1,22	,041	1,000	,00	,999	,467	1,70	0,147
<b>PSI-1</b>	0,151	0,151	0,121	,044	,942	,93	,406	,162	0,067	0,722
<b>Fp1H</b>	0,709	0,848	0,685	,041	,983	,26	,777	,235	0,781	0,157
<b>T5H</b>	0,664	0,840	0,648	,040	,956	,67	,522	,284	0,756	0,169
<b>P3H</b>	0,770	0,845	0,661	,041	,987	,19	,827	,126	0,782	0,159
<b>Age, ys</b>	54,6	48,8	48,1	,039	,955	,68	,512	,691	49,8	0,275

Table 12. Summary of Stepwise Analysis for Variables-Predictors, ranked by criterion Lambda

Variables	F to enter	p-level	$\Lambda$	F-value	p-level
<b>C4H</b>	32,4	$10^{-6}$	,425	32,4	$10^{-6}$
<b>O1H</b>	9,8	$10^{-3}$	,300	19,4	$10^{-6}$
<b>Sex Index</b>	4,0	,026	,255	15,0	$10^{-6}$
<b>T4H</b>	2,9	,064	,226	12,4	$10^{-6}$
<b>F8H</b>	3,8	,031	,193	11,2	$10^{-6}$
<b>PSI-2</b>	3,8	,031	,164	10,5	$10^{-6}$
<b>F7H</b>	4,1	,024	,137	10,2	$10^{-6}$
<b>Fp2H</b>	2,3	,109	,123	9,5	$10^{-6}$
<b>C3H</b>	2,5	,097	,110	9,0	$10^{-6}$
<b>F3H</b>	2,9	,070	,096	8,7	$10^{-6}$
<b>F4H</b>	3,9	,029	,080	8,8	$10^{-6}$
<b>LCG H</b>	2,1	,135	,071	8,5	$10^{-6}$
<b>O2H</b>	1,8	,175	,065	8,1	$10^{-6}$
<b>P4H</b>	1,7	,189	,059	7,8	$10^{-6}$
<b>T3H</b>	1,0	,378	,052	7,0	$10^{-6}$
<b>ICG H</b>	1,6	,215	,047	6,8	$10^{-6}$
<b>HRV H</b>	1,1	,340	,044	6,5	$10^{-6}$
<b>PAI-2</b>	1,0	,379	,041	6,2	$10^{-6}$

The prognostic information is condensed in two roots, including a major 68,3% ( $r^*=0,922$ ; Wilks'  $\Lambda=0,041$ ;  $\chi^2_{(38)}=124$ ;  $p<10^{-6}$ ), a minor 31,7% ( $r^*=0,851$ ; Wilks'  $\Lambda=0,276$ ;  $\chi^2_{(18)}=50$ ;  $p<10^{-4}$ ).

Applying the previous algorithm, we visualize the initial state of each member of the three clusters (Fig. 19) by the raw coefficients and constants in Table 13.

**Table 13. Standardized and Raw Coefficients and Constants for Variables-Predictors**

Coefficients	Standardized		Raw	
	Root 1	Root 2	Root 1	Root 2
<b>C4H</b>	-,691	,010	-7,441	,111
<b>O1H</b>	-,480	,389	-3,540	2,871
<b>Sex Index</b>	-,610	-,723	-1,372	-1,627
<b>T4H</b>	-,795	,541	-7,815	5,325
<b>F8H</b>	1,392	-,805	7,345	-4,248

PSI-2	-,732	-,644	-1,584	-1,393
F7H	-,177	1,516	-,889	7,628
Fp2H	,308	,713	2,506	5,794
C3H	-,528	,651	-5,833	7,191
F3H	,951	-1,046	7,804	-8,582
F4H	-,842	,452	-7,473	4,017
LCG H	-,632	-,188	-13,81	-4,101
O2H	-,654	-,726	-4,487	-4,975
P4H	,517	,604	4,448	5,196
T3H	-,168	-,970	-1,893	-10,96
ICG H	-,120	-,666	-2,053	-11,40
HRV H	,344	,375	2,860	3,119
PAI-2	,157	,351	,431	,962
	<b>Constants</b>		24,91	5,675
	<b>Eigenvalues</b>		5,671	2,628
<b>Cumulative Properties</b>			,683	1,000

As we can see, the normalizing increase of the entropy of SPD EEG in members of the **third cluster**, which localize in the extreme right zone of the axis of the first root, is conditioned by its minimum initial levels (maximum negentropy) at the loci C4, C3, F4, T3 and F3, which is negatively related to the root as well as the maximum for sampling level ICG entropy, which is positively related to the root (Table 14).

Another predictor is gender (6 males out of 7 members), which is quantified by the minimum sex index (male = 1, female = 2). The members of the other two clusters are located in the opposite zone of the axis and their projections are mixed.

These clusters are demarcated along the axis of the second root, which reflects the increased entropy levels of SPD EEG in loci O1, Fp2, F7, F8, O2, T4 and P4 in combination with minimally reduced HRV entropy and maximum reduced Popovych's Adaptation Index-2 in the members of the **first cluster**, whereas in the members of the **second cluster**, the entropy levels of SPD at these loci are reduced and the negentropy of HRV is maximum.

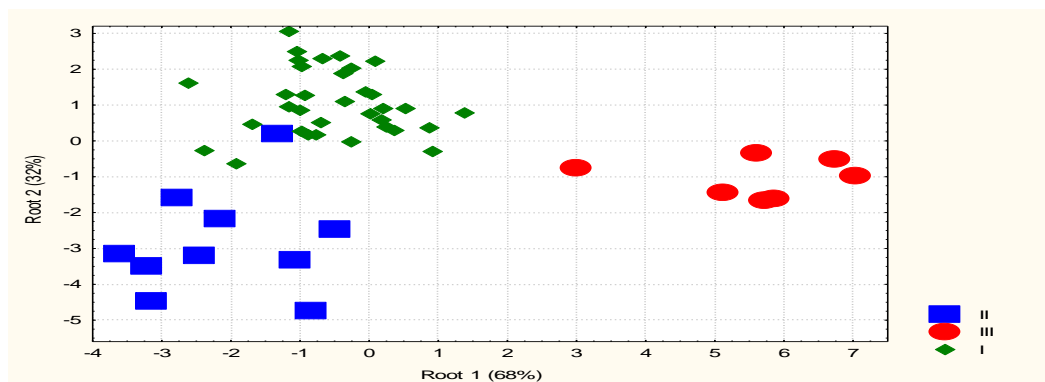


**Fig. 19. Individual values of the two roots of the predictors for the members of the three clusters**

**Table 14. Correlations Variables-Canonical Roots, Means of Roots and Z-scores of Variables-Predictors**

Variables initial	Correlations Variables-Roots		II (10)	I (34)	III (7)
	R 1	R 2			
<b>Root 1 (68,3%)</b>					
C4H	<b>-,481</b>	,120	<b>+0,80</b>	<b>+0,60</b>	<b>-2,59</b>
C3H	<b>-,473</b>	,131	<b>+0,79</b>	<b>+0,64</b>	<b>-2,48</b>
F4H	<b>-,420</b>	,160	<b>+0,09</b>	<b>+0,14</b>	<b>-2,97</b>
T3H	<b>-,391</b>	,101	<b>+0,59</b>	<b>+0,45</b>	<b>-1,82</b>
F3H	<b>-,228</b>	,059	<b>+0,40</b>	<b>+0,30</b>	<b>-1,41</b>
Sex Index	<b>-,076</b>	-,122	<b>0,00</b>	<b>-0,71</b>	<b>-0,95</b>
PSI-2	<b>-,077</b>	-,232	<b>+5,87</b>	<b>+3,32</b>	<b>+1,86</b>
LCG H	<b>-,039</b>	-,123	<b>-0,18</b>	<b>-0,63</b>	<b>-0,85</b>
ICG H	<b>,059</b>	-,118	<b>-0,27</b>	<b>0,00</b>	<b>+0,25</b>
<b>Root 2 (31,7%)</b>					
O1H	,049	<b>,392</b>	<b>-0,51</b>	<b>+0,75</b>	<b>+0,30</b>
Fp2H	,003	<b>,366</b>	<b>-0,83</b>	<b>+0,65</b>	<b>-0,16</b>
F7H	-,015	<b>,298</b>	<b>-1,23</b>	<b>+0,27</b>	<b>-0,71</b>
F8H	,051	<b>,290</b>	<b>-1,08</b>	<b>+0,33</b>	<b>-0,06</b>
O2H	-,018	<b>,287</b>	<b>-0,30</b>	<b>+0,64</b>	<b>0,00</b>
T4H	-,158	<b>,211</b>	<b>-0,02</b>	<b>+0,53</b>	<b>-0,74</b>
P4H	-,147	<b>,196</b>	<b>+0,11</b>	<b>+0,60</b>	<b>-0,54</b>
HRV H	-,009	<b>,053</b>	<b>-1,01</b>	<b>-0,76</b>	<b>-0,97</b>
PAI-2	,046	<b>-,099</b>	<b>-3,36</b>	<b>-4,01</b>	<b>-3,16</b>

In the information space of two roots, all three clusters are delineated very clearly (Fig. 19 and Table 15).

**Table 15. Squared Mahalanobis Distances between Predictors for Clusters of changes in Entropy, F-values (df=19,3) and p-levels**

Clusters	II	III	I
II	0	<b>66</b>	<b>19</b>

III	7,8 <math><10^{-6}</math>	0	44
I	4,4 <math><10^{-3}</math>	7,4 <math><10^{-6}</math>	0

This means that, with the help of predictors and classification functions (Table 16), the identity of a particular person to one or another cluster of entropy changes is almost unmistakable (Table 17).

**Table 16. Coefficients and Constants for Classification Functions for Predictors of Changes in Entropy**

Clusters	II	III	I
<b>Variables</b>	p=,196	p=,137	p=,667
<b>C4H</b>	384,1	327,1	372,8
<b>O1H</b>	249,6	227,5	255,2
<b>Sex Index</b>	21,48	8,00	12,99
<b>T4H</b>	297,8	247,3	306,3
<b>F8H</b>	-236,7	-187,9	-241,7
<b>PSI-2</b>	55,48	40,80	47,56
<b>F7H</b>	-55,26	-48,37	-26,94
<b>Fp2H</b>	-7,88	21,81	18,63
<b>C3H</b>	-126,0	-157,9	-107,1
<b>F3H</b>	-143,3	-98,72	-164,4
<b>F4H</b>	121,95	71,72	125,85
<b>LCG H</b>	1166	1053	1128
<b>O2H</b>	152,8	109,4	126,4
<b>P4H</b>	-389,7	-346,1	-362,4
<b>T3H</b>	381,3	347,1	335,7
<b>ICG H</b>	792,8	756,5	745,2
<b>HRV H</b>	-108,7	-81,10	-92,05
<b>PAI-2</b>	,59	5,63	5,01
<b>Constants</b>	-1038	-847,0	-970,4

**Table 17. Classification Matrix for Predictors of Changes in Entropy**

Rows: Observed classifications; Columns: Predicted classifications

	Percent	II	III	I
Clusters	correct	p=,196	p=,137	p=,667
II	90	<b>9</b>	0	<b>1</b>
III	100	0	<b>7</b>	0
I	100	0	0	<b>34</b>
Total	98	9	7	35

The following article will analyze the associated changes in the immunity parameters specific to each of the three entropy change clusters.

### Acknowledgment

We express sincere gratitude to administration of JSC “Truskavets’ kurort” and “Truskavets’ SPA” as well as clinical sanatorium “Moldova” for help in conducting this investigation.

### Accordance to ethics standards

Tests in patients are conducted in accordance with positions of Helsinki Declaration 1975, revised and complemented in 2002, and directive of National Committee on ethics of scientific researches. During realization of tests from all participants the informed consent is got and used all measures for providing of anonymity of participants.

### Conflicts of interest

The authors declare no conflict of interest. The founders had no role in the design of the study; in the collection, analyses, or interpretation of data; in the writing of the manuscript, or in the decision to publish the results.

### References

- Aldenderfer MS, & Blashfield RK. (1989). Cluster analysis (Second printing, 1985) [trans. from English in Russian]. In: Factor, Discriminant and Cluster Analysis. Moskva. Finansy i Statistika; 139-214.
- Baevskiy RM, & Ivanov GG. (2001). Heart Rate Variability: theoretical aspects and possibilities of clinical application [in Russian]. *Ultrazvukovaya i funktsionalnaya diagnostika*. 3: 106-127.
- Balanovs’kyi VP, Popovych IL, & Karpynets’ SV. (1993). About ambivalence-equilibratory character of influence of curative water Naftussya on organism of human [in Ukrainian]. *Dopovidi ANU. Mat., pryr., tekhn. Nauky*. 3: 154-158.
- Barylyak LG., Malyuchkova RV, Tolstanov OB, Tymochko OB, Hryvna RF, & Uhryn MR. (2013). Comparative estimation of informativeness of leucocytary index of adaptation by Garkavi and by Popovych. *Medical Hydrology and Rehabilitation*. 11(1): 5-20.
- Berntson GG, Bigger JT jr, Eckberg DL, Grossman P, Kaufman PG, Malik M, Nagaraja HN, Porges SW, Saul JP, Stone PH, & Van der Molen MW. (1997). Heart Rate Variability: Origines, methods, and interpretive caveats. *Psychophysiology*. 34: 623-648.



- Chebanenko OI, Flyunt IS, Popovych IL, Balanovs'kyi VP, & Lakhin PV. (1997). Water Naftussya and hydro-mineral exchange [in Ukrainian]. Kyiv: Naukova dumka. 141 p.
- Chebanenko OI, Chebanenko LO, & Popovych IL. (2012). Variety Balneoeffects of Factors Spa Truskavets' and their Forecast [in Ukrainian]. Kyiv: UNESCO-SOCIO. 496 p.
- Gozhenko AI. (2004). Dysregulation as the basis of the pathophysiology of homeostasis [in Ukrainian]. Clinical and experimental pathology. 3(2): 191-193.
- Gozhenko AI. (2010). Essays on disease theory [in Russian]. Odesa; 24 p.
- Gumega MD, Levyts'kyi AB, & Popovych IL. (2011). Balneogastroenterology [in Ukrainian]. Kyiv: UNESCO-SOCIO. 243 p.
- Heart Rate Variability. (1996). Standards of Measurement, Physiological Interpretation, and Clinical Use. Task Force of ESC and NASPE. Circulation. 93(5): 1043-1065.
- Ivassivka SV, Bilas VR, & Popovych AI. (2008). Influence applications of ozokerite on phone of chronic stress on parameters of neuro-endocrine-immune complex and hydro-electrolyte exchange at rats. Communication 1: Stresslimiting, sanogene and neutral effects [in Ukrainian]. Medical Hydrology and Rehabilitation. 6(4): 65-72.
- Ivassivka SV, Bilas VR, & Popovych AI. (2008). Stresslimiting effects of ozokerite on neuro-endocrine-immune complex at rats. In: International Scientific Congress and 61-st Session of the General Assembly of the World Federation of Hydrotherapy Climatotherapy (FEMTEC). Congress materials (China, November 26-28, 2008): 216-217.
- Klecka WR. (1989). Discriminant Analysis [trans. from English in Russian] (Seventh Printing, 1986). In: Factor, Discriminant and Cluster Analysis. Moskva: Finansy i Statistika; 78-138.
- Kolyada TI, Volyanskyi YL, Vasilyev NV, & Maltsev VI. (1995). Adaptation Syndrome and Immunity [in Russian]. Kharkiv: Osnova; 168 p.
- Kostyuk PG, Popovych IL, & Ivassivka SV (editors). (2006). Chernobyl', Adaptive and Defensive Systems, Rehabilitation [in Ukrainian]. Kyiv. Computerpress; 348 p.
- Kozyavkina NV. (2009). Neuro-endocrine and electrolyte accompaniment of multivariate thyrotropic effects of Naftussya bioactive water [in Ukrainian]. Medical Hydrology and Rehabilitation. 7(1): 51-55.
- Kozyavkina NV. (2012). Thyrotropic effects of bioactive water Naftusia in female rats and their metabolic, neuroendocrine and immune accompaniments [in Ukrainian]. Medical Hydrology and Rehabilitation. 10(4): 91-113.
- Kozyavkina NV, Popovych IL, & Zukow W. (2013). Metabolic accompaniment of thyrotropic effects of bioactive water Naftussya at the women with thyroid hyperplasia. Journal of Health Sciences. 3(5): 409-424.
- Kozyavkina OV, Vis'tak HI, & Popovych IL. (2013). Factor, canonical and discriminant analysis of vegetotropic effects and accompanying changes in thyroide, metabolic and haemodynamic parameters at the women, caused by bioactive water Naftussya. Medical Hydrology and Rehabilitation. 11(3): 4-28.
- Kozyavkina OV, Kozyavkina NV, Gozhenko OA, Gozhenko AI, Barylyak LG, & Popovych IL. (2015). Bioactive Water Naftussya and Neuroendocrine-Immune Complex [in Ukrainian]. Kyiv: UNESCO-SOCIO; 349 p.
- Kul'chyns'kyi AB, Zukow W, Korolyshyn TA, & Popovych IL. (2017). Interrelations between changes in parameters of HRV, EEG and humoral immunity at patients with chronic pyelonephritis and cholecystitis. Journal of Education, Health and Sport. 7(9): 439-459.
- Lapovets' LY, & Lutsyk BD. (2002). Handbook of Laboratory Immunology [in Ukrainian]. Lviv. 173 p.
- Petsyukh SV, Petsyukh MS, Kovbasnyuk MM, Barylyak LG, & Zukow W. (2016). Relationships between Popovych's Adaptation Index and parameters of ongoing HRV and EEG in patients with chronic pyelonephrite and cholecystite in remission. Journal of Education, Health and Sport. 6(2): 99-110.

- Popadynets' OO, Gozhenko AI, Zukow W, & Popovych IL. (2019). Relationships between the entropies of EEG, HRV, immunocytogram and leukocytogram. *Journal of Education, Health and Sport*. 9(5): 651-666.
- Popadynets' OO, Gozhenko AI, Zukow W, & Popovych IL. (2019). Interpersonal differences between of the entropies of EEG, HRV, immunocytogram and leukocytogram. *Journal of Education, Health and Sport*. 9(6): 534-545.
- Popadynets' OO, Gozhenko AI, Zukow W, & Popovych IL. (2019). Peculiarities of spectral parameters of EEG, HRV and routine parameters of immunity in patients with various levels of the entropy of EEG, HRV, immunocytogram and leukocytogram. *Journal of Education, Health and Sport*. 9(8): 617-636.
- Popovych AI. (2018). Features of the immunotropic effects of partial components of the balneotherapeutic complex of spa Truskavets'. *Journal of Education, Health and Sport*. 8(12): 919-935.
- Popovych AI. (2019). Features of the neurotropic effects of partial components of the balneotherapeutic complex of spa Truskavets'. *Journal of Education, Health and Sport*. 9(1): 396-409.
- Popovych IL. (2007). Information effects of bioactive water Naftussya in rats: modulation entropic, prevention desynchronizing and limitation of disharmonizing actions water immersion stress for information components of neuro-endocrine-immune system and metabolism, which correlates with gastroprotective effect [in Ukrainian]. *Medical Hydrology and Rehabilitation*. 5(3): 50-70.
- Popovych IL. (2008). Stresslimiting effects of bioactive Naftussya water under chronic restrictive stress in rats [in Ukrainian]. *Medical Hydrology and Rehabilitation*. 6(3): 128-153.
- Popovych IL. (2011). Stresslimiting Adaptogene Mechanism of Biological and Curative Activity of Water Naftussya [in Ukrainian]. Kyiv: Computerpress; 300 p.
- Popovych IL, Gumeza MD, Verba IE, Popovych AI, Korolyshyn TA, Tkachuk SP, Ostapenko VM, & Zukow W. (2016). Comparative investigation effects on nervous and immune systems of bioactive water Naftussya spa Truskavets' and stable water solution of Boryslav's ozokerite. *Journal of Education, Health and Sport*. 6 (4): 364-374.
- Popovych IL, & Kozyavkina NV. (2012). Metabolic accompaniment of thyrotropic effects of bioactive water Naftussya in women with thyroid hyperplasia [in Ukrainian]. *Medical Hydrology and Rehabilitation*. 10(4): 114-138.
- Popovych IL, Kul'chyns'kyi AB, Gozhenko AI, Zukow W, Kovbasnyuk MM, Korolyshyn TA. (2018). Interrelations between changes in parameters of HRV, EEG and phagocytosis at patients with chronic pyelonephritis and cholecystitis. *Journal of Education, Health and Sport*. 8(2): 135-156.
- Popovych IL, Kul'chyns'kyi AB, Korolyshyn TA, & Zukow W. (2017). Interrelations between changes in parameters of HRV, EEG and cellular immunity at patients with chronic pyelonephritis and cholecystitis. *Journal of Education, Health and Sport*. 7(10): 11-23.
- Popovych IL, Ruzhylo SV, Ivassivka SV, & Aksentiychuk BI (editors). (2005). *Balneocardioangiology* [in Ukrainian]. Kyiv: Computerpress. 229 p.
- Popovych IL, Vis'tak HI, Gumeza MD, & Ruzhylo SV. (2014). *Vegetotropic Effects of Bioactive Water Naftussya and their Endocrine-Immune, Metabolic and Hemodynamic Accompaniments* [in Ukrainian]. Kyiv: UNESCO-SOCIO; 163 p.
- Ruzhylo SV, Tserkovnyuk AV, & Popovych IL. (2003). *Actotropic Effects of Balneotherapeutic Complex of Truskavets spa* [in Ukrainian]. Kyiv: Computerpress; 131 p.
- Shannon CE. (1963). *Works on the theory of informatics and cybernetics* [transl. from English to Russian]. Moskwa: Inostrannaya literatura; 329 p.
- Sydoruk NO, Chebanenko OI, Popovych IL, & Zukow W. (2017). *Comparative Investigation of Physiological Activity of Water Naftussya from Truskavets' and Pomyarky Deposits* [in Ukrainian]. Kyiv: UNESCO-SOCIO; 216 p.

Yushkova OG. (2001). Using information theory to study adaptive responses in the body athletes [in Ukrainian]. *Medical Rehabilitation, Kurortology, Physiotherapy*. 1(25): 40-43.

Zukow W, Popadynets' OO, Gozhenko AI, & Popovych IL. (2019). Interindividual differences in parameters of the EEG and HRV in the humans with various levels of the entropy of EEG, HRV, immunocytogram and leukocytogram. *Journal of Education, Health and Sport*. 9(7): 448-466.